Macular Dystrophy and Cone-Rod Dystrophy Caused by Mutations in the *RP1* Gene: Extending the *RP1* Disease Spectrum

Sanne K. Verbakel,[1] Ramon A. C. van Huet,[1] Anneke I. den Hollander,[1,2] Maartje J. Geerlings,[1] Eveline Kersten,[1] B. Jeroen Klevering,[1] Caroline C. W. Klaver,[1,3,4] Astrid S. Plomp,[5] Nieneke L. Wesseling,[6] Arthur A. B. Bergen,[5,7] Konstantinos Nikopoulos,[8,9] Carlo Rivolta,[8,10] Yasuhiro Ikeda,[11] Koh-Hei Sonoda,[11] Yuko Wada,[12] Camiel J. F. Boon,[6,13] Toru Nakazawa,[14,15] Carel B. Hoyng,[1] and Koji M. Nishiguchi[14,15]

[1]Department of Ophthalmology, Donders Institute for Brain, Cognition and Behavior, Radboud University Medical Center, Nijmegen, The Netherlands
[2]Department of Human Genetics, Donders Institute for Brain, Cognition and Behavior, Radboud University Medical Center, Nijmegen, The Netherlands
[3]Department of Ophthalmology, Erasmus Medical Center, Rotterdam, The Netherlands
[4]Department of Epidemiology, Erasmus Medical Center, Rotterdam, The Netherlands
[5]Department of Clinical Genetics, Amsterdam UMC, University of Amsterdam, Amsterdam, The Netherlands
[6]Department of Ophthalmology, Amsterdam UMC, University of Amsterdam, Amsterdam, The Netherlands
[7]The Netherlands Institute for Neuroscience (NIN-KNAW), Amsterdam, The Netherlands
[8]Department of Computational Biology, Unit of Medical Genetics, University of Lausanne, Lausanne, Switzerland
[9]Service of Medical Genetics, Lausanne University Hospital (CHUV), Lausanne, Switzerland
[10]Department of Genetics and Genome Biology, University of Leicester, Leicester, United Kingdom
[11]Department of Ophthalmology, Graduate School of Medical Sciences, Kyushu University, Fukuoka, Japan
[12]Yuko Wada Eye Clinic, Sendai, Japan
[13]Department of Ophthalmology, Leiden University Medical Center, Leiden, The Netherlands
[14]Department of Advanced Ophthalmic Medicine, Tohoku University Graduate School of Medicine, Sendai, Japan
[15]Department of Ophthalmology, Tohoku University Graduate School of Medicine, Sendai, Japan

Correspondence: Carel B. Hoyng, Department of Ophthalmology, Radboud University Medical Center, P.O. Box 9101, Nijmegen 6500 HB, The Netherlands;
Carel.Hoyng@radboudumc.nl.

PURPOSE. To describe the clinical and genetic spectrum of *RP1*-associated retinal dystrophies.

METHODS. In this multicenter case series, we included 22 patients with *RP1*-associated retinal dystrophies from 19 families from The Netherlands and Japan. Data on clinical characteristics, visual acuity, visual field, ERG, and retinal imaging were extracted from medical records over a mean follow-up of 8.1 years.

RESULTS. Eleven patients were diagnosed with autosomal recessive macular dystrophy (arMD) or autosomal recessive cone-rod dystrophy (arCRD), five with autosomal recessive retinitis pigmentosa (arRP), and six with autosomal dominant RP (adRP). The mean age of onset was 40.3 years (range 14–56) in the patients with arMD/arCRD, 26.2 years (range 18–40) in adRP, and 8.8 years (range 5–12) in arRP patients. All patients with arMD/arCRD carried either the hypomorphic p.Arg1933* variant positioned close to the C-terminus (8 of 11 patients) or a missense variant in exon 2 (3 of 11 patients), compound heterozygous with a likely deleterious frameshift or nonsense mutation, or the p.Gln1916* variant. In contrast, all mutations identified in adRP and arRP patients were frameshift and/or nonsense variants located far from the C-terminus.

CONCLUSIONS. Mutations in the *RP1* gene are associated with a broad spectrum of progressive retinal dystrophies. In addition to adRP and arRP, our study provides further evidence that arCRD and arMD are *RP1*-associated phenotypes as well. The macular involvement in patients with the hypomorphic *RP1* variant suggests that macular function may remain compromised if expression levels of RP1 do not reach adequate levels after gene augmentation therapy.

Keywords: RP1, phenotypic spectrum, macular dystrophy, cone-rod dystrophy, retinitis pigmentosa

R etinitis pigmentosa (RP) encompasses a heterogeneous group of inherited retinal dystrophies characterized by rod photoreceptor degeneration that precedes cone photoreceptor degeneration. The *RP1* gene is one of the more than 80 genes associated with RP. Besides *RP1*, seven other RP genes—*BEST1*, *NR2E3*, *NRL*, *RHD12*, *RHO*, *RPE65*, and *SAG*—have been associated with both autosomal dominant and autosomal recessive modes of inheritance.[1] In general, RP patients with

an autosomal recessive inheritance pattern have a more severe disease course compared with patients with autosomal dominant RP (adRP). This also applies to patients with *RP1*-associated RP: autosomal recessive *RP1* patients generally have a lower age of onset compared with autosomal dominant *RP1* patients, as well as a worse long-term prognosis with respect to retaining central vision due to the occurrence of early macular atrophy or cystoid macular edema.[1,2]

The *RP1* gene, mapped to chromosome 8q12.1, contains four exons, three of which are coding, and encodes a photoreceptor-specific microtubule-associated protein that plays a vital role in the architecture of both rod and cone photoreceptor outer segments.[3,4] RP1 is located at the photoreceptor axoneme, where it links outer segment discs to the axonemal microtubules, and thereby regulates the length and stability of the axoneme.[5] The interaction with the microtubules is mediated primarily by two doublecortin (DCX) domains encoded by exons 2 and 3.[5] In addition, RP1 contains a third putative domain, between amino acid residues 486 and 635, that shares homology with the *Drosophila melanogaster* bifocal (BIF) protein, which is required for normal photoreceptor morphogenesis.[6] *RP1* mutations that are known to cause adRP are clustered in a relatively small region in exon 4 between amino acid residues 500 and 1053,[7] and result in the production of a truncated protein with a presumed dominant-negative activity.[8] In contrast, most mutations located more toward the N- or C-terminus of RP1 result in autosomal recessive RP (arRP).[7]

In 2016, Ellingford et al.[9] identified compound heterozygous mutations in *RP1* (i.e., p.Tyr41His and p.Leu172Arg) in a patient diagnosed with macular dystrophy (MD)/presumed Stargardt disease. However, because this new genotype-phenotype correlation was identified in only a single family, they concluded that reevaluation of the clinical phenotype was warranted.[9] Knowledge about the entire disease spectrum associated with certain genes is important, particularly in view of novel therapeutic options, as the prognosis and disease course between phenotypes may differ markedly. In this study, we report patients diagnosed with MD and cone-rod dystrophy (CRD) in addition to patients with RP, and expand the clinical spectrum associated with mutations in the *RP1* gene.

METHODS

Patients

Twenty-two patients (19 families) with a retinal dystrophy and mutations in the *RP1* gene were clinically examined at the Radboud university medical center in Nijmegen, The Netherlands (families A, B, M, N , P, and Q); the Tohoku University Graduate School of Medicine in Sendai, Japan (families C–E, J and L); the Kyushu University Hospital, Fukuoka, Japan (families F and K); the Yuko Wada Eye Clinic, Sendai, Japan (family G); and the Amsterdam UMC, The Netherlands (families H, I, O, R and S). The genetic evaluation was performed between June 2013 and May 2018. Informed consent was obtained from all patients before data collection and additional ophthalmic examinations. The study adhered to the tenets of the Declaration of Helsinki, and was approved by the local ethics committees.

Genetic Analysis

In all families, genomic DNA was extracted from peripheral lymphocytes according to standard procedures. The genetic data of the Japanese patients was obtained in context of another study.[10] In short, whole exome sequencing was performed in patients A-II:2, A-II:4, A-II:5, B-II:8, H-II:2, I-II:2, M-II:2, P-II:13, and Q-III:4. The exome data were analyzed using a vision gene panel consisting of 220 (patients H-II:2 and I-II:2), 342 (patient P-II:13), 366 (patient B-II:7), and 395 genes (patients M-II:2 and Q-III:4) or without the use of a gene filter (family A). See Supplementary Table S1 for an overview of the genes included in these panels. Targeted panel sequencing covering 256 (patient R-IV:2) or 266 vision genes (patients O-II:1 and S-III:4) was performed in a certified DNA diagnostic laboratory, with additional Sanger sequencing for all areas with a coverage below 30 reads (Supplementary Table S1). Mutational screening in patient N-III:9 was performed using an arrayed primer extension microarray for adRP (containing 414 variants in 16 genes), according to a previously described protocol.[11] All variants detected by microarray analysis were verified by direct sequencing. Patients C to G and J to L had their *RP1* open reading frame screened by means of Sanger sequencing as previously reported.[10] In addition, molecular inversion probes were used to exclude variants in 109 other inherited retinal dystrophy genes in patients C to F, J, and K,[10] and targeted resequencing containing 83 nonsyndromic RP genes was performed in patient L-II:2 (Supplementary Table S1). The pathogenicity of novel missense variants was assessed combining cosegregation analysis and in silico prediction tools, including SIFT and Polyphen-2, and by using the PhyloP, CADD-PHRED, and Grantham scores. For an extensive description of the genetic analysis, see Supplement 1.

Clinical Evaluation

Clinical data were obtained from the medical records of the patients. In addition, three patients (family A) were reevaluated after the identification of the causative *RP1* mutations. We performed a detailed ophthalmic examination, which included visual acuity testing, slit-lamp biomicroscopy, and detailed ophthalmoscopy. Most patients also underwent conventional fundus photography and/or ultra-widefield fundus imaging (Optos P200Tx; Optos, Dunfermline, UK), Goldmann perimetry, as well as spectral-domain optical coherence tomography (SD-OCT) using a confocal scanning laser ophthalmoscope (Spectralis HRA+OCT; Heidelberg Engineering, Heidelberg, Germany; Cirrus; Carl Zeiss Meditec, Inc., Dublin, CA; or Topcon 3D OCT-2000; Topcon, Inc, Tokyo, Japan). Fundus autofluorescence (FAF) imaging was performed using the Spectralis HRA+OCT 30° × 30° field of view centered on the macula,[12] or the 200° field of view from the ultra-widefield imaging device. All patients underwent full-field ERG, and multifocal electroretinography (mfERG) was performed in patients B-II:8, C-II:2, D-II:1, and E-II:2. Electrophysiological recordings were performed according to the International Society for Clinical Electrophysiology of Vision guidelines and assessed by applying local standard values.[13,14]

Patients were diagnosed based on their (initial) symptoms, fundus abnormalities, ERG findings, and overall course of the disease. They received the diagnosis MD if they experienced central vision loss without symptoms of night blindness, ophthalmoscopy and multimodal imaging revealed no signs of peripheral involvement, in the presence of an intact peripheral visual field, normal to marginally abnormal scotopic ERG responses, and normal to moderately reduced photopic ERG responses. Patients with a panretinal phenotype received the diagnosis CRD or RP, depending on which photoreceptor function was affected first. CRD was diagnosed when the onset of loss of central vision preceded that of night blindness, presence of a central scotoma, no or mild constriction of the visual field, and reduced ERG responses in a cone-rod pattern. Patients were diagnosed with RP when they presented with night blindness, constriction of the visual field, and reduced

ERG responses in a rod-cone pattern. The clinical distinction between MD and CRD, however, can be difficult and is sometimes arbitrary in view of the significant clinical overlap. In addition, in individual MD patients the MD may progress in a more generalized disorder that fits the criteria of CRD. In the present study, we therefore grouped the MD and CRD spectrum into a single category for further analysis.

RESULTS

Genetic Findings

Genetic analysis detected 16 unique variants in the *RP1* gene, including six newly identified variants, in the 19 families (Fig. 1).[10] The novel variants included five nonsense and frameshift mutations, as well as the p.Val190Gly missense variant that is likely pathogenic according to the guideline proposed by the American College of Medical Genetics and Genomics.[15] The variant segregates with the disease (M8, family H), affects a highly conserved amino acid that is located in the DCX domain, is extremely rare in the gnomAD database (1/249046), and is predicted to be pathogenic with a high Grantham score (109/215) and CADD-PRHED score (22.2) including a high SIFT (pathogenic) and PolyPhen-2 score (probably damaging). Heterozygous variants in other inherited retinal dystrophy genes are listed in Supplementary Table S2.

Notably, compound heterozygous mutations were identified in all patients with autosomal recessive MD (arMD)/autosomal recessive CRD (arCRD). In particular, the p.Arg1933* mutation, which was identified in a compound heterozygous state with another nonsense or frameshift mutation in six of eight families with arMD/arCRD, from both East Asian and Caucasian origins (Fig. 1). The remaining two families with arMD/arCRD (families B and H) carried a heterozygous missense mutation (p.Phe180Cys or p.Val190Gly) located in exon 2, in the region that encodes the DCX domain, together with a frameshift mutation on the second allele. Families with an identical combination of mutations were identified; p.Arg1933* in combination with p.Tyr1352Alafs*9 was previously identified in four families of East Asian origin (families C– F).[10]

In contrast, in five of six families with arRP, homozygous nonsense or frameshift variants were identified. Remarkably, the p.Tyr1352Alafs*9 mutation that was found in patients with arMD/arCRD in combination with p.Arg1933* in families C to F, was identified in a homozygous state in two families with arRP (families J and K), as described.[10] In addition, the p.Pro124Alafs*20 mutation that causes arMD/arCRD in combination with the p.Val190Gly missense mutation in patient H, was also identified in a homozygous state in arRP family N.

Clinical Findings

An overview of the individual clinical characteristics of the patients with an *RP1* mutation is provided in the Table. The clinical characteristics stratified by phenotype are provided in Supplementary Table S3. Of the 22 patients, 11 patients (7 arMD and 4 arCRD patients from eight families) were diagnosed with arMD/arCRD, 5 patients (five families) with arRP, and 6 patients (six families) with adRP. Patient B-II:8 was initially diagnosed with a hydroxychloroquine-associated maculopathy as she received treatment with hydroxychloroquine for rheumatoid arthritis. The correct diagnosis of *RP1*-associated MD was made based on her clinical presentation that was atypical for hydroxychloroquine maculopathy, the low cumulative dose of 280 g of hydroxychloroquine, and an affected sister free of the medication. Subsequent molecular genetic testing revealed compound heterozygous mutations in the *RP1* gene in both of them.

Patients With arMD/arCRD

The patients with arMD/arCRD presented the latest of the three phenotypes (mean age of onset 40.3 years; SD 13.1 years, range 14–56 years), although they showed overlap in age at onset with the adRP patients (mean 26.2 years, SD 8.2 years, range 18–40 years, $P = 0.025$) (Supplementary Table S3). Their initial symptom was a decrease in visual acuity or metamorphopsia, sometimes accompanied by photophobia (patient C-II:2) or night blindness (patient F-II:3 and G-II:2). With progression of the disease, 8 of 11 patients developed photophobia. All patients were myopic (range of spherical equivalents: −9.50 diopters [D] to −0.25 D). Biomicroscopy revealed several types of lens opacities in 6 of 11 patients of whom patient F-II:3 underwent cataract extraction at the age of 61 years (Table, Supplementary Table S3). The course of the visual acuity for each patient is represented in Figure 2. Ten patients revealed mild to moderate visual acuity impairment during working life, which eventually led to acuity levels of 20/400 in the eighth decade (patient A-II:2). However, patient C-II:2 already had a visual acuity of 20/400 at the age of 41 years. Visual field testing revealed an absolute central scotoma, except for a paracentral scotoma in the left eye of patient B-II:8 (age 55 years), and a central, relative scotoma in patient B-II:3 (age 64 years). In addition, the visual field was mildly constricted in patients B-II:3, F-II:3, and G-II:2.

Ophthalmoscopy showed RPE alterations or atrophy in the macula (Table, Fig. 3). Attenuation of the retinal vessels was present in patients A-II:4, B-II:3, F-II:3, and G-II:2, focal bone spicule pigmentations were observed in patient F-II:3, and a single nummular pigmentation in patient G-II:2. A bull's eye maculopathy was noticed in the left eye of patient B-II:8 (age 55) and both eyes of patient E-II:2 at the most recent examination. In patient A-II:5, the bull's eye maculopathy had progressed to macular atrophy with foveal involvement (Fig. 4). A posterior staphyloma was visible in patient A-II:2 with spherical equivalents of −8.38/−8.00 D. SD-OCT images revealed loss of the outer retinal layers in the macula, with sparing of the foveal photoreceptors in the patients with a bull's eye maculopathy and the left eye of patient B-II:3 (age 64), in which the photoreceptors and RPE at the fovea were preserved in a foveal sparing-like pattern (Fig. 3F). The right eye of patient B-II:3 initially showed foveal sparing at the age of 56 years, although shortly afterward the foveal cells degenerated as well, with a corresponding loss in visual acuity. FAF imaging showed a round to oval zone of reduced FAF or a speckled pattern of alternating normal and decreased FAF, bordered by a band of increased FAF (Fig. 3); except for patient E:II-2, in whom an oval zone of increased FAF was visible without a reduced autofluorescence signal. FAF images of patients F-II:3 and G-II:2 were not acquired. Full-field ERG ranged from normal rod and cone responses to patients in whom both cone and rod responses were moderately or severely reduced (Table). The mfERG, performed in patients B-II:8, C-II:2, D-II:1, and E-II:2, was severely reduced in all patients except for patient B-II:8 in whom a decreased response in the parafoveal ring was visible in the right eye and moderately reduced responses in the left eye.

Autosomal Recessive RP

The arRP patients were affected at the earliest age, with a mean age of onset of 8.8 years and an onset at the age of only 5 years in the youngest patient (SD 2.8; range 5–12 years; Supplementary Table S3). The initial symptom in the arRP patients was
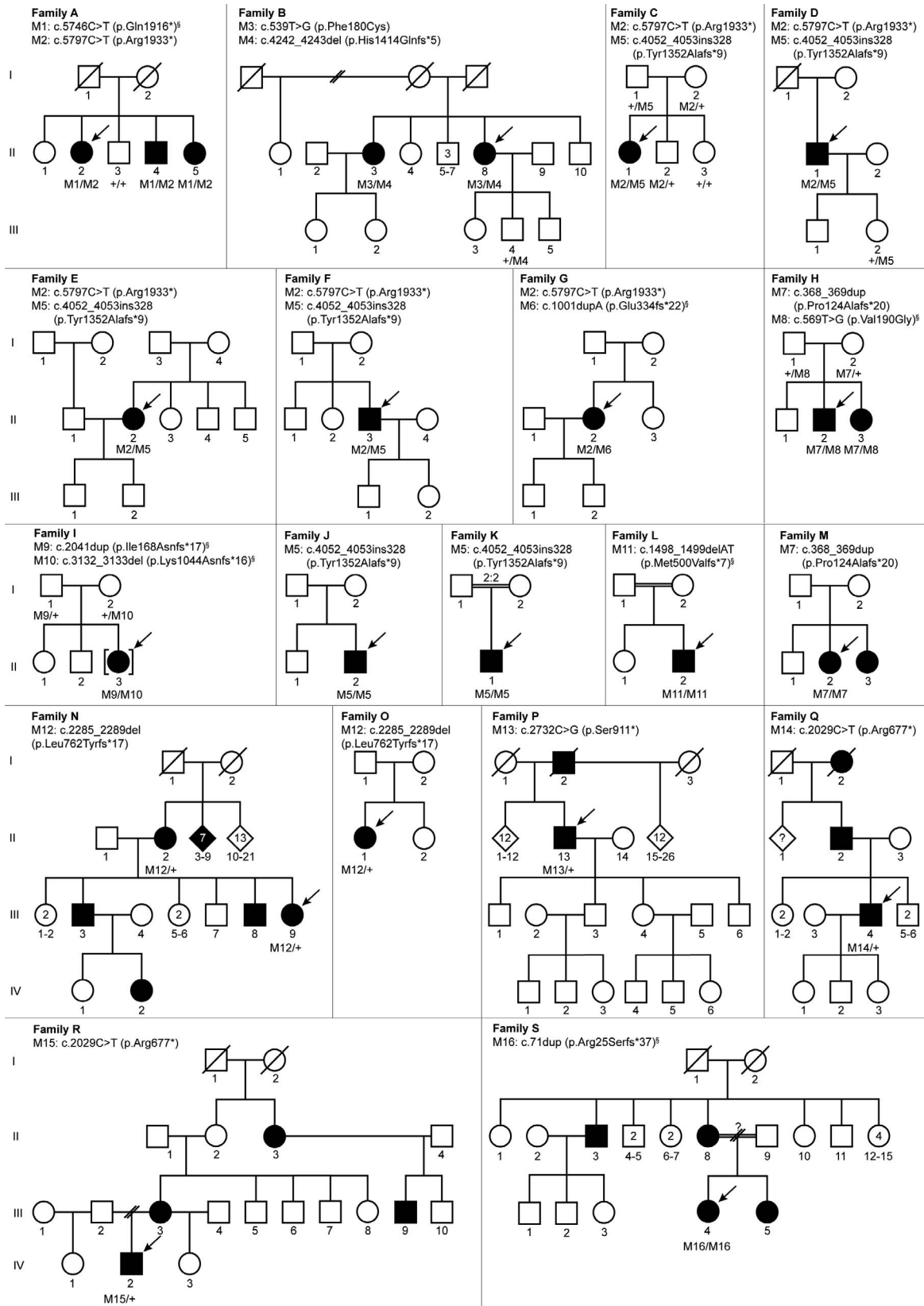
FIGURE 1. Pedigrees of the families included in this study. *Squared boxes* indicate men, *circles* indicate women, *filled symbols* represent affected persons, and *unfilled symbols* represent unaffected persons. The plus sign denotes the wild-type allele, and the *arrow* indicates the proband of the family. *Double lines* point out consanguineous marriages, the number above the lines indicates the degree of consanguinity. Where relatives were available (families A, B, C, D, H, I, and N), the mutations segregate with the disease. Families C to F, J, and K have previously been described by Nikopoulos et al.[10] §Novel variants.

Investigative Ophthalmology & Visual Science

TABLE. Clinical Features of Patients Carrying Pathogenic Mutations in *RP1*

| ID/Sex/Age of Onset, y/Age Race	Initial Symptom	Visual Acuity RE LE	SER† RE LE	Lens Status	Ophthalmoscopy Results	ERG Results Scot	Phot	Goldmann Perimetry	Dx	Mutation(s)
MD/CRD										
A-II:2/F/31/77 Caucasian	Decrease in VA/ metamorphopsia	20/400 20/400	−8.38 −8.00	Mild PSC, severe cortical and nuclear cataract	Well-demarcated area of central and peripapillary chorioretinal atrophy. Normal aspect of retinal vessels and optic disc. Posterior staphyloma LE>RE.	SN	MR	Central scotoma	arMD	p.Gln1916* p.Arg1933*
A-II:4/M/50/69 Caucasian	Decrease in VA	20/200 20/200	−2.00 −2.00	Cortical and nuclear cataract	Well-demarcated area of central and peripapillary chorioretinal atrophy. Normal optic disc, mild attenuation of retinal veins. No intraretinal hyperpigmentation.	N	N	Central scotoma	arMD	p.Gln1916* p.Arg1933*
A-II:5/F/45/67 Caucasian	Metamorphopsia	20/500 20/63	−5.50 −4.88	Cortical and nuclear cataract, mild PSC	Macular and peripapillary atrophy. Normal aspect of vasculature and optic disc. No intraretinal hyperpigmentation.	N	N	Central scotoma	arMD	p.Gln1916* p.Arg1933*
B-II:3/F/56/64 Caucasian	Decrease in VA	20/110 20/125	−2.00 −1.00	Mild cortical and nuclear cataract	Severe atrophy and gliosis in the macula BE, with foveal sparing in the LE. Peripapillary atrophy, attenuated vessels, and no intraretinal hyperpigmentation.	SR	SR	Slightly constricted VF (RE>LE), moderate central sensitivity loss	arCRD	p.Phe180Cys p.His1414Glnfs*5
B-II:8/F/55/55 Caucasian	Decrease in VA	20/400 20/17	−1.00 −0.50	Clear	Well-demarcated area of macular atrophy in the RE, and RPE alterations with a bull's eye configuration in the LE. Normal aspect of the retinal vessels and optic disc. No intraretinal hyperpigmentation.	N	SN	Central scotoma RE, paracentral scotoma LE	arMD	p.Phe180Cys p.His1414Glnfs*5
C-II:2/F/25/41 East Asian	Decrease in VA/ photophobia	20/500 20/400	−9.00 −9.50	Clear	RPE alterations in the macula with small, parafoveal areas of atrophy. Normal aspect of the optic disc and retinal vessels. No intraretinal hyperpigmentation.	SN	MR	Central scotoma	arMD	p.Arg1933* p.Tyr1352Alafs*9
D-II:1/M/44/54 East Asian	Decrease in VA	20/222 20/133	−2.50 −2.50	Clear	RPE alterations in the macula with small, parafoveal areas of RPE atrophy. Peripapillary atrophy. Normal aspect of the optic disc and retinal vessels. No intraretinal hyperpigmentation.	SN	MR	Central scotoma	arMD	p.Arg1933* p.Tyr1352Alafs*9

Investigative Ophthalmology & Visual Science

TABLE. Continued

ID/Sex/Age of Onset, y/Age Race	Initial Symptom	Visual Acuity RE / LE	SER† RE / LE	Lens Status	Ophthalmoscopy Results	ERG Results Scot	ERG Results Phot	Goldmann Perimetry	Dx	Mutation(s)
E-II:2/F/36/43 East Asian	Decrease in VA	20/33 / 20/50	−0.25 / −0.25	Clear	Granular pigment alterations in the macula in a bull's eye pattern. Normal aspect of the optic disc and retinal vessels. No intraretinal hyperpigmentation.	SN	MR	Central scotoma	arMD	p.Arg1933* / p.Tyr1352Alafs*9
F-II:3/M/50/61 East Asian	Decrease in VA/ night blindness	20/630 / 20/400	−0.50 / −2.50	Moderate cortical and mild nuclear cataract; extracted at 60y	Macular atrophy, mild attenuation of retinal vessels, nummular hyperpigmentation LE.	MR	MR	Central scotoma and mild VF constriction	arCRD	p.Arg1933* / p.Tyr1352Alafs*9
G-II:2/F/37/37 East Asian	Decrease in VA/ night blindness	20/50 / 20/200	−1.25 / −1.00	Clear	Macular atrophy, mild attenuation of retinal vessels. Sporadic nummular pigmentation in LE.	SR	SR	Central scotoma and VF constriction (nasal>temporal)	arCRD	p.Arg1933* / p.Glu334fs*22
H-II:2/M/14/18 Caucasian	Decrease in VA	20/28 / 20/50	−3.00 / −2.00	Clear	Mild RPE alterations in the macula. Periphery normal.	MR	MR	Intact peripheral VF	arCRD	p.Pro124Alafs*20 / p.Val190Gly
arRP										
I-II:3/F/11/13 Caucasian	Night blindness	20/25 / 20/22	−2.13 / −1.63	Unknown	Bone spicule pigmentation, attenuated vessels, pallor op the optic disc, and peripheral atrophy.	NR	SR	Constricted VF to 10–15°	arRP	p.Ile168Asnfs*17 / p.Lys1044Asnfs*16
J-II:2/M/6/32 Caucasian	Night blindness	20/67 / LP	−4.00 / −4.50	Mild nuclear cataract	Macular atrophy, attenuation of retinal vessels, bone spicule pigmentation, and pallor of the optic disc.	NR	NR	Constricted VF <10°	arRP	p.Tyr1352Alafs*9 / p.Tyr1352Alafs*9
K-II:1/M/12/46 East Asian	Night blindness	HM / HM	−1.25 / −2.00	PSC and ASC; extracted at 45y	Profound panretinal degeneration, abundant bone spicule pigmentation, and severely attenuated vessels. Vascular sheathing LE.	NP	NP	Constricted VF <10°	arRP	p.Tyr1352Alafs*9 / p.Tyr1352Alafs*9
L-II:2/M/10/22 East Asian	Night blindness	20/67 / 20/50	−5.50 / −5.25	Congenital coronary cataract BE	Bone spicule pigmentation, attenuated retinal vessels, pallor of the optic disc, and central RPE alterations with small islands of macular atrophy.	SR	SR	Constricted VF <10°	arRP	p.Met500fs*33 / p.Met500fs*33
M-II:2/F/5/52 Caucasian	Night blindness	LP / LP	−9.00 / −8.25	Mild PSC, mild cortical and nuclear cataract	Generalized retinal dystrophy with macular atrophy, bone spicule pigmentation, attenuated retinal vessels, and waxy pallor of the optic disc.	NR (46y)	NR (46y)	No VF measurable	arRP	p.Pro124Alafs*20 / p.Pro124Alafs*20

Investigative Ophthalmology & Visual Science

TABLE. Continued

ID/Sex/Age of Onset, y/Age Race	Initial Symptom	Visual Acuity RE LE	SER† RE LE	Lens Status	Ophthalmoscopy Results	ERG Results Scot	Phot	Goldmann Perimetry	Dx	Mutation(s)
adRP										
N-II:9/F/18/56 East Asian	Night blindness	20/50 20/50	−9.38 −10.00	Moderate nuclear cataract; extracted at 55y	Tessellated fundus with RPE atrophy in the periphery, dense nummular and bone spicule pigmentation, severely attenuated retinal vessels, and waxy pallor of the optic disc.	NR (51y)	NR (51y)	Constricted VF to 10° with a small temporal residue	adRP	p.Leu762Tyrfs*17
O-II:1/F/ childhood/40 Caucasian	Night blindness	20/66 20/40	−5.75 −5.50	Mild cataract	Profound atrophy with some sparing of the center, bone spicule pigmentation, attenuated retinal vessels, and pallor of the optic disc.	NR (36y)	SR (36y)	Constricted VF to 10°, with a inferonasal residue (RE) and temporal residue (LE)	adRP	p.Leu762Tyrfs*17
P-II:13/M/40/72 Caucasian	Night blindness	20/40 20/63	+1.50 +4.00	Moderate nuclear cataract; extracted at 70y	Profound (mid)peripheral atrophy, extensive bone spicule and nummular pigmentation, severe attenuation of retinal vessels, and waxy pallor of the optic disc.	NR (71y)	NR (71y)	Constricted VF to 15° (RE) and 20° (LE)	adRP	p.Ser911*
Q-III:4/M/25/46 African	Night blindness	20/55 20/46	−4.00 −4.00	Extracted at 34y	Profound bone spicule pigmentations, severe attenuation of retinal vessels, peripapillary atrophy and some (waxy) pallor of the optic disc.	NR	NR	Constricted VF to 5° (RE) and 3° (LE)	adRP	p.Arg677*
R-IV:2/M/25/35 Caucasian	Night blindness	20/20 20/20	−1.25 −2.25	Clear	Bone spicule pigmentation in the midperiphery (particularly nasal retina), mild attenuation of the retinal vessels, normal aspect of the optic disc. Mild ERM right eye.	NP	NP	Constricted VF <10°	adRP	p.Arg677*
S-III:4/F/23/40 Caucasian	Night blindness	20/20 20/34	−3.38 −3.38	Clear	Bone spicule pigmentation, attenuated retinal vessels, generalized retinal atrophy with foveal sparing.	NR	SR	HFA 30–2: central residue	adRP	p.Arg25Serfs*37

All features are present symmetrically, unless mentioned otherwise. ASC, anterior subcapsular cataract; BE, both eyes; Dx, final diagnosis; ERM, epiretinal membrane; F, female; HFA, Humphrey field analyzer; HM, hand movements; LE, left eye; LP, light perception; M, male; MR, moderately reduced; N, normal; NP, not performed; NR, nonrecordable; Phot, photopic; PSC, posterior subcapsular cataract; RE, right eye; SER, spherical equivalent refraction; Scot, scotopic; SN, subnormal; SR, severely reduced; VA, visual acuity; VF, visual field.
† If cataract surgery has been performed, the preoperative spherical equivalent was reported.
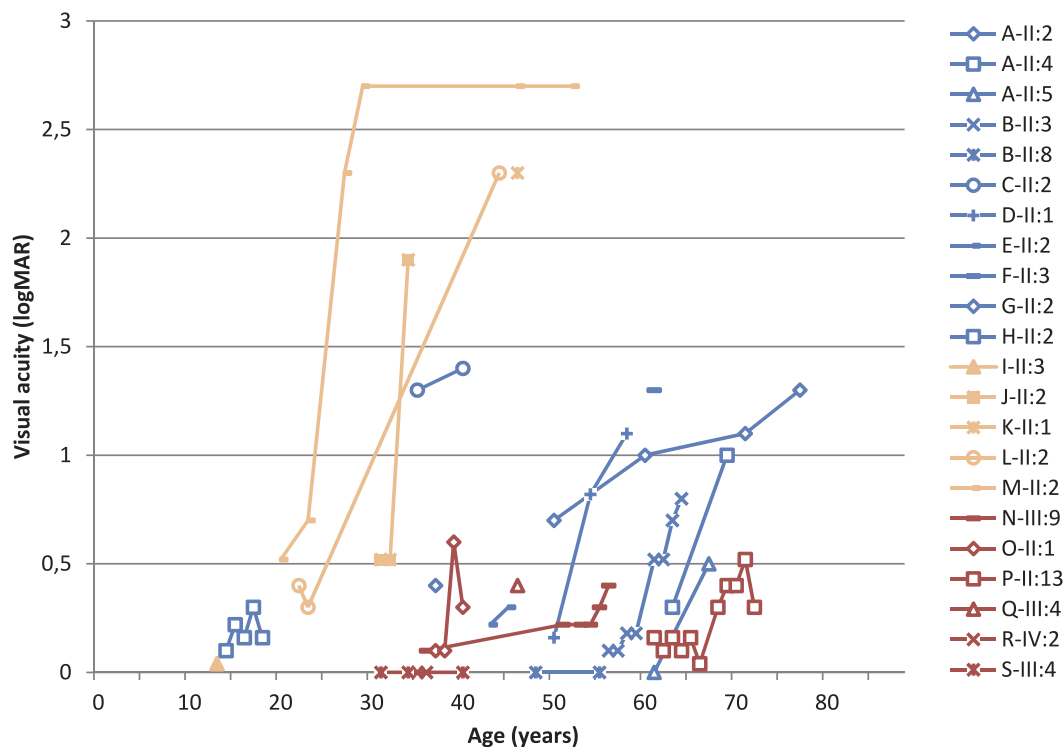
FIGURE 2. Graph showing the course of visual acuity over time in patients with mutations in the *RP1* gene. The three phenotypes are indicated with different colors: arMD/arCRD in *blue*, arRP in *orange*, and adRP in *red*. The visual acuity of the best eye is displayed. Snellen visual acuity was converted into logMAR. A logMAR value of 1.9 was assigned to counting fingers (CF), 2.3 to hand movements (HM), and 2.7 to light perception (LP).

night blindness in all cases and all patients were myopic (range of spherical equivalents: −9.00 D to −1.63 D; Table, Supplementary Table S3). Despite their young age, all four patients for whom data were available already showed lens opacities at a mean age of 33 years. The visual acuity deteriorated from adolescence or early adulthood to levels of light perception in the sixth decade of life and constriction of the visual field with a residue of less than 10 degrees at the most recent examination was present in three of four patients (Table, Fig. 2).

Ophthalmoscopy showed the three hallmark RP signs—bone spicule pigmentations, attenuation of the retinal vessels, and pallor of the optic disc—often accompanied by profound peripheral RPE atrophy. In addition, macular atrophic lesions were present in four of five patients, with sparing of the fovea in two of them (Table). This was confirmed by an intact ellipsoid zone layer in the fovea on SD-OCT (Fig. 3R, Supplementary Table S3). Finally, ERG responses were severely reduced or nonrecordable under scotopic and photopic conditions in all RP patients.

Autosomal Dominant RP

Patients with adRP presented with night blindness, at a mean age of 26.2 years (SD 8.2; range 18–40 years). Five of six patients were myopic (range of spherical equivalents: −10.00 to +4.00), except for patient O-II:13, who was hyperopic with spherical equivalents of +1.50 D and +4.00 D (Table). Biomicroscopy revealed several types of lens opacities in four of six patients of whom three patients underwent cataract extraction (Table, Supplementary Table S3). The visual acuity was relatively preserved, as all patients retained a visual acuity of 20/80 or better, even at the age of 72 (patient O-II:13) (Fig. 2, Supplementary Table S3). However, the visual field showed severe constriction with a central residue of less than 10

degrees in two of six patients at a mean age of 48 years (Table, Supplementary Table S3).

The patients with adRP also showed bone spicule pigmentation and attenuation of the retinal vessel, often accompanied by profound peripheral RPE atrophy and macular atrophy in four of six patients (Table). However, the fovea was spared from the atrophic lesions in all patients (except for the left eye of patient O-II:1). Patient O-II:1 previously underwent a pars plana vitrectomy with peeling of the internal limiting membrane in both eyes for macular holes. Cystoid macular edema was present in patient Q-III:4, with a moderate response to oral carbonic anhydrase inhibitors. Finally, ERG responses were nonrecordable under scotopic conditions and severely reduced or nonrecordable under photopic conditions.

DISCUSSION

Mutations in the *RP1* gene have previously been described in patients with adRP and arRP. In the present study, we provide a detailed clinical description of these phenotypes and report two additional *RP1*-associated diagnoses: arMD and arCRD, which may represent a single spectrum of retinal degeneration.

The patients with *RP1*-associated arMD/arCRD presented with a decrease in visual acuity or metamorphopsia, generally first noticed in the fourth decade, which eventually progressed to legal blindness. Considerable macular abnormalities were observed at the most recent examination including a bull's eye maculopathy in two patients. This bull's eye maculopathy may eventually progress to macular atrophy with foveal involvement, as was observed in patient A-II:5. Unfortunately, longitudinal data of the other patients to confirm this hypothesis were not available.

MD and CRD may show large overlap in clinical and genetic findings. This overlap also occurs in time: an MD phenotype
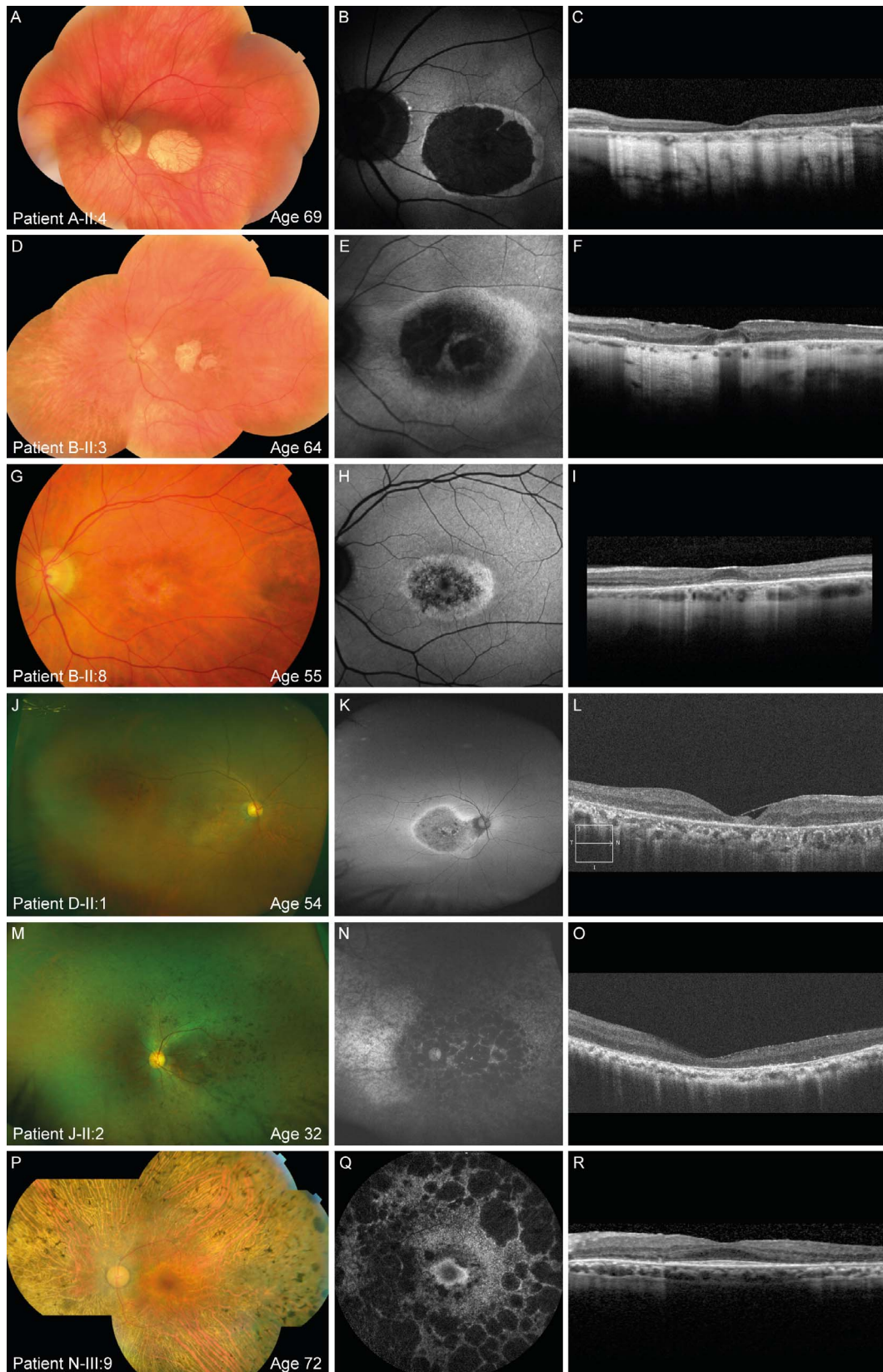
FIGURE 3. Multimodal images of patients with mutations in *RP1*. (**A–C**) Multimodal images of the left eye of patient A-II:4. (**A**) Composite fundus photograph showing a well-demarcated area of chorioretinal atrophy involving the fovea. (**B**) This area corresponds with an oval zone of absent FAF, bordered by a small residual band of increased FAF. (**C**) SD-OCT scan revealing loss of the outer retinal layers in the macula. (**D–F**) Multimodal imaging of the left eye of patient B-II:3. (**D**) Composite fundus photograph showing macular atrophy, attenuated retinal vessels, and no hyperpigmentation. (**E**) FAF image revealing decreased autofluorescence surrounded by a hyperautofluorescent ring. (**F**) SD-OCT scan showing

preservation of the RPE, ellipsoid zone, and external limiting membrane layer in the fovea, and an epiretinal membrane. (**G–I**) Multimodal imaging of the left eye of patient B-II:8, at the age of 55 years. (**G**) Fundus photograph showing a bull's eye maculopathy, a normal aspect of the optic disc and vasculature, and no intraretinal hyperpigmentation. (**H**) FAF shows a corresponding oval area of speckled hyper- and hypoautofluorescence, surrounded by a ring of hyperautofluorescence. (**I**) SD-OCT image revealing the parafoveal loss of outer retinal layers with preservation of the ellipsoid zone and external limiting membrane layer in the fovea. (**J–L**) Multimodal imaging of the right eye of patient D-II:1. (**J**) Ultra-widefield fundus photograph showing RPE alterations in the macula, peripapillary atrophy, no hyperpigmentations, and a normal aspect of the optic disc and retinal vessels. (**K**) Ultra-widefield FAF image showing a speckled pattern of hyper- and hypoautofluorescence, surrounded by a band of increased FAF. (**L**) OCT scan showing generalized loss of photoreceptor inner and outer segments, and an epiretinal membrane. (**M–O**) Multimodal imaging of the left eye of patient J-II:2. (**M**) Ultra-widefield fundus photograph showing RPE atrophy, bone spicule pigmentation, and attenuation of the retinal vessels. (**N**) Autofluorescence image revealing decreased autofluorescence in the macula and along and surrounding to the vascular arcades. (**O**) SD-OCT scan showing generalized loss of the outer retinal layers in the macula. (**P–R**) Multimodal imaging of the left eye of patient N-III:9. (**P**) Composite fundus photograph showing profound peripheral atrophy, severe attenuation of retinal vessels, extensive bone spicule and nummular pigmentation, and waxy pallor of the optic disc. (**Q**) FAF image showing a hyperautofluorescent ring in the macula, surrounded by a speckled pattern of hyper- and hypoautofluorescence, and nummular areas of decreased macular and peripheral autofluorescence. (**R**) SD-OCT scan revealing the preservation of the photoreceptor layer at the fovea.

can eventually progress to a more generalized disorder and converge into a CRD phenotype. This may explain the intrafamilial differences in family B, as patient B-II:8 shows abnormalities limited to the macular region, whereas her older sister displays generalized disease, which may represent a later disease stage. It might also explain the more severe phenotype in patient F-II:3, who carries the same mutations as the younger patients C to E with less severe disease. In addition, the mean age of onset of both phenotypes was the same ($P = 0.817$). Therefore, arMD and arCRD might represent the longitudinal progression of macular/cone predominant *RP1*-associated disease. Nevertheless, some patients may never show progression to a CRD phenotype and other (genetic) modifiers may also exert their effect on the final phenotype. Because the focus of our manuscript lies on the description of patients with a phenotype that does not match the existing phenotypes with predominant rod involvement, we have combined them into the all-embracing term "arMD/arCRD."

The arMD/arCRD shows similarities with other MDs (e.g., central areolar choroidal dystrophy and Stargardt disease),

multifocal pattern dystrophy simulating Stargardt disease, and cone dystrophies, and, because of its later age of onset, can mimic AMD.[16–18] It is, however, important to distinguish these disorders to provide the patient with valuable and correct prognostic information and accurate treatment. An adequate family history, the absence of drusen, and the symmetrical presentation of the macular atrophy can help the clinician in distinguishing hereditary forms of MDs from AMD.[17] The absence of irregular yellowish (pisciform) and/or hyperautofluorescent flecks can help to differentiate *RP1*-associated disease from Stargardt disease, pseudo-Stargardt, and certain cases of central areolar choroidal dystrophy, and ERG responses can help to differentiate from cone dystrophies.

The phenotype of the RP patients was in accordance with earlier reports on RP caused by *RP1* mutations in literature. The five patients with arRP experienced night blindness in the first or second decade of life and showed early involvement of the macular region, whereas the age of onset in the six patients with adRP was between the second and fourth decades, and the fovea remained relatively intact during the course of the
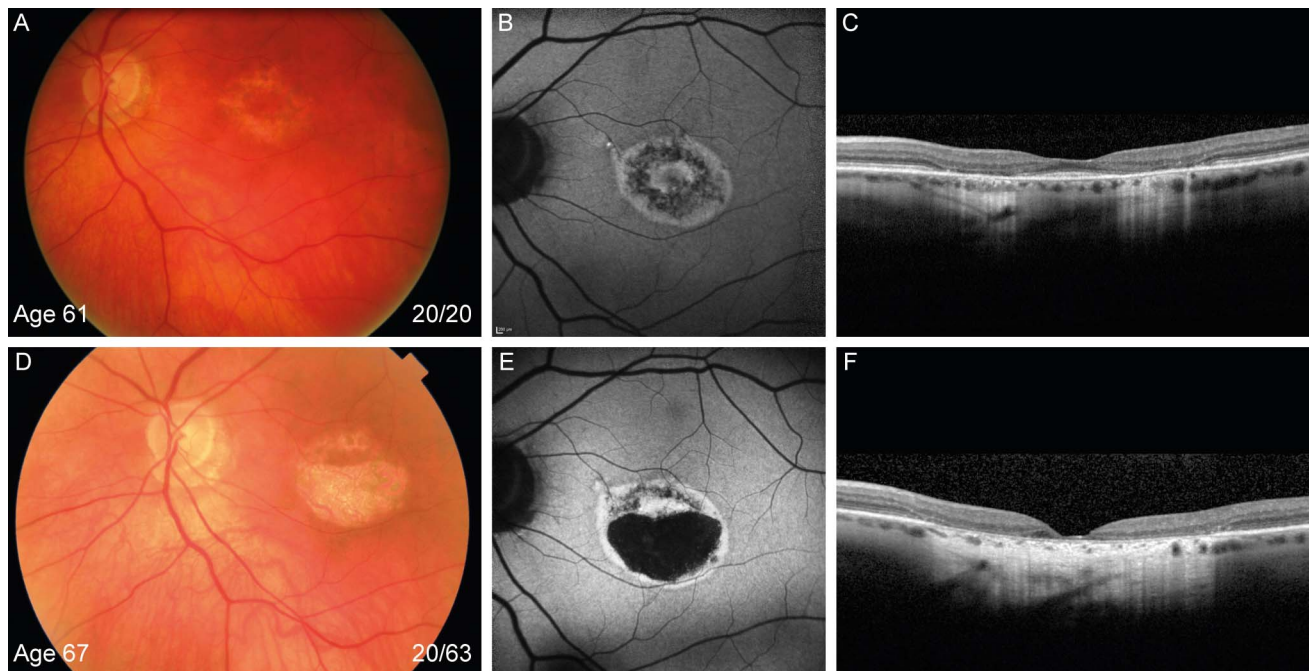
FIGURE 4. Multimodal images of the left eye of patient A-II:5 over an interval of 6 years. (**A**) Fundus photograph showing a bull's eye maculopathy, some peripapillary atrophy, and a normal aspect of the optic disc and retinal vessels. (**B**) The FAF image reveals an oval area of hyperautofluorescence containing a ring of hyper- and hypoautofluorescence. (**C**) Horizontal SD-OCT showing perifoveal loss of the outer retinal layers. (**D**) Fundus photograph 6 years later showing macular atrophy, and (**E**) FAF showing the corresponding area of hypoautofluorescence surrounded by a zone of increased autofluorescence. (**F**) The OCT scan shows the loss of the outer retinal layers that now also involves the fovea.

disease.[1,2] Myopia, in varying degrees, is a common feature, and was found in 96% of patients. This association of myopia and *RP1*-related disease has previously been described, particularly in arRP patients.[19,20]

Together, these four retinal dystrophies now form the spectrum of *RP1*-associated disease. It is, however, important to realize that the RP phenotypes are not simply a more extensive form of the more centrally located form of *RP1*-associated disease. This is illustrated by the visual acuity in the adRP patients that can remain relatively preserved even in advanced RP cases as well as the different predominantly affected photoreceptors

The phenotype is, to a large extent, determined by the location and severity of the mutations in the *RP1* gene. Several classifications of mutations have been proposed.[7,21,22] In Supplementary Figure S1, we provide the latest overview of mutations and their location. The mutations responsible for adRP reside in a hotspot region in exon 4 between amino acid residues 500 and 1053, and are expected to result in a truncated protein with dominant-negative activity.[8] In contrast, arRP is caused by the presence of two nonsense or frameshift mutations in *RP1*. Patients with arMD/arCRD carry a heterozygous variant that is expected to have a mild effect on protein function (p.Phe180Cys, p.Val190Gly, or p.Arg1933*) in combination with a more severe nonsense or frameshift mutation, or a combination of two predicted mild variants such as p.Gln1916* and p.Arg1933* in family 1 and the compound heterozygous missense variants (p.Tyr41His and p.Leu172Arg) reported by Ellingford et al.[9] in a single MD patient (Fig. 1). The p.Arg1933* variant, a recurrent variant in the Japanese population (allele frequency: 0.6%), does not cause a retinal dystrophy in homozygous carriers, at least not before the age of 80 years.[10] Although, in combination with a pathogenic variant, such as p.Glu334fs*22, p.Tyr1352Alafs*9, or another likely hypomorphic variant p.Gln1916*, the effect of this hypomorphic allele seems to be sufficient to cause retinal disease (Fig. 1).

Although these findings are consistent within our study, there are reports, albeit with limited clinical information, that conflict with our findings. For example, p.Arg1933* was found in trans with the p.Tyr834* nonsense variant in a patient with arRP.[23] In addition, other previously reported variants, such as p.D202E, p.I1988Nfs*3, and p.I2061Sfs*12, could also be predicted to be mild or hypomorphic variants considering their location; however, they have been associated with arRP, although the clinical phenotype has not been described in detail.[23–25] The explanation for this clinical heterogeneity remains to be elucidated, but might be explained by additional (genetic-) modifying factors, the presence of a structural variant or a variant in the non-coding regions of *RP1*, pathogenic variants in another RP gene, or inaccurate phenotyping, the latter of which should be considered particularly in advanced RP and CRD, in which the distinction can be difficult and depends on patients' self-reported disease course. A potential genetic modifier for *RP1*-associated disease may be RP1L1, because these proteins have synergistic roles in the photoreceptor axoneme.[26] However, we did not find any rare variants in the *RP1L1*, although intronic or structural variants cannot be excluded (Supplementary Table S2).

RP1 is an interesting candidate for gene therapy, because of its relatively high prevalence in RP.[1] However, important challenges must be overcome before gene therapy for *RP1* can reach the clinic. For example, knowledge about the natural course of the disease is required to be able to evaluate treatment efficacy, particularly in view of the different phenotypes. In addition, in case of gene augmentation therapy, the maximum cargo capacity of the AAVs (~4.7 kb) is too limited to fit the *RP1* gene (6.5 kb),[27,28] and the optimal expression levels of the RP1 protein need to be determined.[8] This could be more important than previously anticipated if our hypothesis that a hypomorphic variant in combination with a deleterious variant causes arMD/arCRD is correct. Insufficient dosage of the *RP1* gene by gene transfer may mimic this condition and could in that case result in the development of an iatrogenic MD. Obviously, this would be a serious concern when treating arRP patients with preserved macular function with the goal to halt the progression of central visual field loss. Although patients with adRP might also benefit from an elevation of wild-type RP1 levels,[8] the mutant protein that possesses dominant-negative activity remains present in the cell and competes with the wild type. Therefore, other genetic therapies, such as treatment with antisense oligonucleotides, of which proof-of-concept has been shown in an animal model with *RHO*-associated RP,[29] or genome editing may be alternative approaches.

In conclusion, mutations in the *RP1* gene can lead to different clinical phenotypes, varying from RP to arMD/arCRD, depending on the residual *RP1* function. Together, these dystrophies form a spectrum of *RP1*-associated phenotypes that can be clinically distinguished from each other based on the clinical findings, inheritance pattern, age of onset, and disease course. However, additional longitudinal studies are essential to improve the diagnostic process and to study the role of potential modifiers. With the advent of novel therapeutic options such as gene therapy, recognition of the entire clinical spectrum associated with *RP1* mutations is essential to aid the selection of patients eligible for treatment, and to evaluate the effect of the treatment provided.

Disclosure: **S.K. Verbakel**, None; **R.A.C. van Huet**, None; **A.I. den Hollander**, None; **M.J. Geerlings**, None; **E. Kersten**, None; **B.J. Klevering**, None; **C.C.W. Klaver**, None; **A.S. Plomp**, None; **N.L. Wesseling**, None; **A.A.B. Bergen**, None; **K. Nikopoulos**, None; **C. Rivolta**, None; **Y. Ikeda**, None; **K.-H. Sonoda**, None; **Y. Wada**, None; **C.J.F. Boon**, None; **T. Nakazawa**, None; **C.B. Hoyng**, None; **K.M. Nishiguchi**, None

References

1. Verbakel SK, van Huet RAC, Boon CJF, et al. Non-syndromic retinitis pigmentosa. *Prog Retin Eye Res*. 2018;66:157–186.

2. Lafont E, Manes G, Senechal A, et al. Patients with retinitis pigmentosa due to RP1 mutations show greater severity in recessive than in dominant cases. *J Clin Exp Ophthalmol*. 2011;2:194.

3. Liu Q, Lyubarsky A, Skalet JH, Pugh EN Jr, Pierce EA. RP1 is required for the correct stacking of outer segment discs. *Invest Ophthalmol Vis Sci*. 2003;44:4171–4183.

4. Gao J, Cheon K, Nusinowitz S, et al. Progressive photoreceptor degeneration, outer segment dysplasia, and rhodopsin

mislocalization in mice with targeted disruption of the retinitis pigmentosa-1 (Rp1) gene. *Proc Natl Acad Sci U S A*. 2002;99:5698–5703.

5. Liu Q, Zuo J, Pierce EA. The retinitis pigmentosa 1 protein is a photoreceptor microtubule-associated protein. *J Neurosci*. 2004;24:6427–6436.

6. Pierce EA, Quinn T, Meehan T, McGee TL, Berson EL, Dryja TP. Mutations in a gene encoding a new oxygen-regulated photoreceptor protein cause dominant retinitis pigmentosa. *Nat Genet* 1999;22:248–254.

7. Siemiatkowska AM, Astuti GD, Arimadyo K, et al. Identification of a novel nonsense mutation in RP1 that causes autosomal recessive retinitis pigmentosa in an Indonesian family. *Mol Vis*. 2012;18:2411–2419.

8. Liu Q, Collin RW, Cremers FP, den Hollander AI, van den Born LI, Pierce EA. Expression of wild-type Rp1 protein in Rp1 knock-in mice rescues the retinal degeneration phenotype. *PLoS One*. 2012;7:e43251.

9. Ellingford JM, Barton S, Bhaskar S, et al. Molecular findings from 537 individuals with inherited retinal disease. *J Med Genet*. 2016;53:761–767.

10. Nikopoulos K, Cisarova K, Quinodoz M, et al. A frequent variant in the Japanese population determines quasi-Mendelian inheritance of rare retinal ciliopathy. *bioRxiv*. 2018. Available at: https://doi.org/10.1101/257634. Accessed November 15, 2018.

11. Zernant J, Kulm M, Dharmaraj S, et al. Genotyping microarray (disease chip) for Leber congenital amaurosis: detection of modifier alleles. *Invest Ophthalmol Vis Sci*. 2005;46:3052–3059.

12. Pichi F, Abboud EB, Ghazi NG, Khan AO. Fundus autofluorescence imaging in hereditary retinal diseases. *Acta Ophthalmol*. 2017;96:e549–e561.

13. Hood DC, Bach M, Brigell M, et al. ISCEV standard for clinical multifocal electroretinography (mfERG) (2011 edition). *Doc Ophthalmol*. 2012;124:1–13.

14. McCulloch DL, Marmor MF, Brigell MG, et al. ISCEV Standard for full-field clinical electroretinography (2015 update). *Doc Ophthalmol*. 2015;130:1–12.

15. Richards S, Aziz N, Bale S, et al. Standards and guidelines for the interpretation of sequence variants: a joint consensus recommendation of the American College of Medical Genetics and Genomics and the Association for Molecular Pathology. *Genet Med*. 2015;17:405–424.

16. Boon CJ, van Schooneveld MJ, den Hollander AI, et al. Mutations in the peripherin/RDS gene are an important cause of multifocal pattern dystrophy simulating STGD1/fundus flavimaculatus. *Br J Ophthalmol*. 2007;91:1504–1511.

17. Saksens NT, Fleckenstein M, Schmitz-Valckenberg S, et al. Macular dystrophies mimicking age-related macular degeneration. *Prog Retin Eye Res*. 2014;39:23–57.

18. Roosing S, Thiadens AA, Hoyng CB, Klaver CC, den Hollander AI, Cremers FP. Causes and consequences of inherited cone disorders. *Prog Retin Eye Res*. 2014;42:1–26.

19. Chassine T, Bocquet B, Daien V, et al. Autosomal recessive retinitis pigmentosa with RP1 mutations is associated with myopia. *Br J Ophthalmol*. 2015;99:1360–1365.

20. Berson EL, Grimsby JL, Adams SM, et al. Clinical features and mutations in patients with dominant retinitis pigmentosa-1 (RP1). *Invest Ophthalmol Vis Sci*. 2001;42:2217–2224.

21. Chen LJ, Lai TY, Tam PO, et al. Compound heterozygosity of two novel truncation mutations in RP1 causing autosomal recessive retinitis pigmentosa. *Invest Ophthalmol Vis Sci*. 2010;51:2236–2242.

22. Avila-Fernandez A, Corton M, Nishiguchi KM, et al. Identification of an RP1 prevalent founder mutation and related phenotype in Spanish patients with early-onset autosomal recessive retinitis. *Ophthalmology*. 2012;119:2616–2621.

23. Li S, Yang M, Liu W, et al. Targeted next-generation sequencing reveals novel RP1 mutations in autosomal recessive retinitis pigmentosa. *Genet Test Mol Biomarkers*. 2018;22:109–114.

24. Mendez-Vidal C, Bravo-Gil N, Gonzalez-Del Pozo M, et al. Novel RP1 mutations and a recurrent BBS1 variant explain the co-existence of two distinct retinal phenotypes in the same pedigree. *BMC Genet*. 2014;15:143.

25. Aldahmesh MA, Safieh LA, Alkuraya H, et al. Molecular characterization of retinitis pigmentosa in Saudi Arabia. *Mol Vis*. 2009;15:2464–2469.

26. Yamashita T, Liu J, Gao J, et al. Essential and synergistic roles of RP1 and RP1L1 in rod photoreceptor axoneme and retinitis pigmentosa. *J Neurosci*. 2009;29:9748–9760.

27. Carvalho LS, Vandenberghe LH. Promising and delivering gene therapies for vision loss. *Vision Res*. 2015;111:124–133.

28. Wu Z, Yang H, Colosi P. Effect of genome size on AAV vector packaging. *Mol Ther*. 2010;18:80–86.

29. Murray SF, Jazayeri A, Matthes MT, et al. Allele-specific inhibition of rhodopsin with an antisense oligonucleotide slows photoreceptor cell degeneration. *Invest Ophthalmol Vis Sci*. 2015;56:6362–6375.